ELSEVIER

Biochimica et Biophysica Acta 1417 (1999) 191–201

BIOCHIMICA ET BIOPHYSICA ACTA
BBA

Contact hypersensitivity: a simple model for the characterization of disease-site targeting by liposomes

Sandra K. Klimuk [a,*], Sean C. Semple [c], Peter Scherrer [c], Michael J. Hope [b,c]

[a] *Department of Biochemistry and Molecular Biology, University of British Columbia, Vancouver, B.C., Canada*
[b] *Division of Dermatology, University of British Columbia, Vancouver, B.C., Canada*
[c] *Inex Pharmaceuticals Corp., Burnaby, B.C., Canada*

Received 23 September 1998; accepted 21 December 1998

Abstract

A murine model of delayed-type hypersensitivity (DTH) is characterized with respect to liposome accumulation at a site of inflammation. Mice were sensitized by painting the abdominal region with a solution of 2,4-dinitrofluorobenzene (DNFB) and inflammation was induced 5 days later by challenging the ear with a dilute solution of DNFB. The inflammatory response was readily monitored by measuring ear thickness (edema) and radiolabeled leukocyte infiltration. Maximum ear swelling and cellular infiltration occurred 24 h after the epicutaneous challenge with the ear returning to normal size after approximately 72 h. We demonstrate that large unilamellar vesicles (LUV) accumulate at the site of inflammation to a level more than 20-fold higher than that measured in the untreated ear. Vesicle delivery to the ear correlated with increased vascular leakage resulting from endothelium remodeling in response to DNFB challenge, and was not a consequence of increased local tissue blood volume. Extravasation occurred only during the first 24 h after ear challenge; after this time the permeability of the endothelium to vesicles returned to normal. We further showed that LUV with a diameter of 120 nm exhibit maximum levels of accumulation, that a polyethylene glycol surface coating does not increase delivery, and that the process can be inhibited by the application of topical corticosteroids at the time of induction. These data and the inflammation model are discussed with respect to developing lipid-based drug delivery vehicles designed to accumulate at inflammatory disease sites.

Keywords: Contact hypersensitivity; Delayed-type hypersensitivity; Extravasation; Inflammation; Liposome; Targeting

1. Introduction

The accumulation of liposomal drug delivery systems within tumors and sites of inflammation or infection is well documented. This phenomenon of disease-site targeting is believed to play a major role in

Abbreviations: AUC, area under the curve; CH, cholesterol; CHE, cholesterylhexadecylether; DNFB, 2,4-dinitrofluorobenzene; DSPC, distearylphosphatidylcholine; DTH, delayed-type hypersensitivity; EPC, egg phosphatidylcholine; HBS, Hepes-buffered saline; ICAM-1, intercellular adhesion molecule-1; LUV, large unilamellar vesicle; MLV, multilamellar vesicle; PBS, phosphate-buffered saline; PEG, polyethylene glycol; PEG-CerC_{20}, 1-*O*-(2′-(ω-methoxypolyethyleneglycol) succinoyl)-2-*N*-arachidoylsphingosine; QELS, quasi-elastic light scattering; SUV, small unilamellar vesicle

* Corresponding author. Present address: Inex Pharmaceuticals Corp., 100–8900 Glenlyon Parkway, Burnaby, B.C. V5J 5J8, Canada. Fax: +1-604-419-3203; E-mail: sklimuk@inexpharm.com

0005-2736/99/$ – see front matter
PII: S0005-2736(98)00261-2

the enhanced efficacy observed for a variety of drugs when formulated inside lipid vesicles [1–4]. Lipid-based formulations of the anthracyclines daunomycin and doxorubicin [4,5] have been in clinical use for several years now, and exhibit markedly improved therapeutic profiles over the free drug. A more recent example is vincristine, a vinca alkaloid commonly used to treat lymphatic malignancies, which exhibits dramatically enhanced efficacy and modestly reduced toxicity when administered in sphingomyelin/cholesterol large unilamellar vesicles (LUV) [6,7]. In general, the pharmacodynamics of liposomal drug delivery to tumors in animal models is well characterized [8–14]; however, less is known about the extravasation of lipid vesicles into areas of inflammation.

In this study we have characterized a murine model of inflammation with respect to liposome accumulation that is based on a delayed-type hypersensitivity (DTH) response to cutaneous contact with the chemical irritant, 2,4-dinitrofluorobenzene (DNFB) [15,16]. As DNFB diffuses across the stratum corneum and into the epidermis, it reacts with amino acid side chains of cell surface proteins. These hapten-modified self proteins are processed by antigen-presenting cells resident in the skin, primarily Langerhans cells and to some extent epidermal keratinocytes. The Langerhans cells migrate from the epidermis via the dermal lymphatic vessels to regional lymph nodes where they mature into interdigitating dendritic cells, which express high levels of MHC class II molecules. These specialized antigen-presenting cells stimulate naive T-cells ($CD4^+$) to differentiate into effector and memory lymphocytes, which circulate through the blood and peripheral tissues. A second cutaneous exposure to DNFB stimulates hapten-specific T-lymphocytes residing in the dermis to release proinflammatory cytokines, initiating a localized inflammatory response at the challenge site. A cascade of events then occurs, resulting in a temporary remodeling of the local dermal vasculature that allows leakage of macromolecules and extravasation of cells into the peripheral tissue. These inflammatory events can generally be measured in terms of four basic endpoints: erythema (redness), edema (swelling), vascular leak (of proteins and small molecules), and cellular infiltration (neutrophils, monocytes, and T cells) [15–17].

One of the primary inflammatory events initiated by the second DNFB exposure is an increased expression of intercellular adhesion molecule-1 (ICAM-1) on the luminal surface of local endothelial cells, keratinocytes, and antigen-presenting cells in the dermis. This protein assists in antigen presentation to T lymphocytes and enhances leukocyte trafficking to the inflammation site by binding circulating leukocytes to the walls of local blood vessels [18]. Diapedesis and migration of leukocytes into the extravascular tissue follow, and it is at this phase of the inflammatory process that lipid vesicles would be expected to extravasate. This model provides a rapid and useful tool to investigate and optimize liposomal formulations with respect to extravasation and disease-site accumulation. Furthermore, we intend to employ this model to evaluate the delivery and efficacy of liposomal formulations of novel anti-inflammatory therapeutics, including antisense oligonucleotides and plasmids.

2. Materials and methods

2.1. Chemicals and lipids

Distearylphosphatidylcholine (DSPC) and egg phosphatidylcholine (EPC) were purchased from Avanti Polar Lipids (Pelham, AL, USA). Cholesterol (CH), dexamethasone, and 2,4-dinitrofluorobenzene (DNFB) were purchased from Sigma (St. Louis, MO, USA). 1-*O*-(2′-(ω-methoxypolyethyleneglycol)-succinoyl)-2-*N*-arachidoylsphingosine (PEG-CerC_{20}) was kindly synthesized by Dr. Zhao Wang (Inex Pharmaceuticals, Burnaby, B.C., Canada). [^{14}C]- and [^{3}H]cholesterylhexadecylether (CHE), [^{3}H]methyl thymidine, and the tissue solubilizer Solvable were obtained from Dupont NEN (Boston, MA, USA). All reagents were used without further purification.

2.2. Mice

Female 8-week-old (25 g) ICR mice were obtained from Harlan Sprague–Dawley and quarantined for 1 week prior to use. Each experimental group consisted of at least four mice.

2.3. Sensitization and initiation of inflammation

The abdominal region of ICR mice was shaved using an electric razor. Mice were sensitized by applying 25 μl of 0.5% DNFB in a vehicle of acetone/olive oil (4:1, v/v) to the shaved abdominal wall for two consecutive days [15]. Four days after the second application, mice were lightly anesthetized with a gas inhalant (halothane) before being challenged on the dorsal surface of the left ear with 10 μl of 0.2% DNFB in the same vehicle. Mice received no treatment on the right ear. In some cases control mice received 10 μl of vehicle on the dorsal surface of the left ear.

2.4. Evaluation of ear swelling

Baseline ear thickness measurements were obtained on anesthetized mice immediately prior to DNFB ear challenge. Thickness measurements were made using an engineer's micrometer (Mitutoyo, Tokyo, Japan), with care being taken to measure only the outer two-thirds of the ear, avoiding skin folds located at the base. Measurements were taken in quadruplicate and the thickness expressed as the mean ± standard deviation. At various time intervals after ears were challenged with DNFB, mice were reanesthetized and their ear thickness was measured. Care was taken not to overly compress the swollen ear between each of the quadruplicate measurements. The average increase in ear thickness was determined by subtracting the baseline measurements from post-challenge measurements.

2.5. Evaluation of cellular infiltration

All mice received a 500 μl intraperitoneal (i.p.) injection of [^{3}H]methyl thymidine in sterile saline (1 μCi/g of body weight) 24 h before the ear was painted with DNFB [19]. After ear thickness measurements were recorded, ears were excised above the major ear fold. Ear tissue was digested whole in 500 μl of Solvable for 12–48 h at 60°C. Samples were then decolorized as described by Longman et al. [10] and analyzed for radiolabeled leukocytes by standard liquid scintillation counting. A relative estimate of cellular infiltration was determined by expressing the ratio of the radioactivity observed in the inflamed versus noninflamed ears.

2.6. Evaluation of liposome accumulation

Large unilamellar vesicles (LUV) composed of DSPC/CH (55:45 molar ratio) or DSPC/CH/PEG-CerC_{20} (45:45:10) were prepared in Hepes-buffered saline (20 mM Hepes, 145 mM NaCl, pH 7.4) by extrusion through two stacked polycarbonate filters of defined pore sizes, as described by Hope et al. [20]. Filter pore sizes were typically 100 nm in diameter unless otherwise indicated. Small unilamellar vesicles (SUV) composed of DSPC/CH (55:45) were prepared by probe sonication using a Branson microtip sonifier. Vesicle sizes were determined by quasi-elastic light scattering (QELS) using a Nicomp Model 370 submicron particle sizer (Pacific Scientific, Santa Barbara, CA, USA). All liposome preparations contained the nonexchangeable lipid marker [^{14}C]- or [^{3}H]CHE. Vesicles were administered at a dose of 100 mg/kg (200 μl; ~2 μCi of CHE per mouse) via the lateral tail vein after initiation of ear inflammation. At various times, mice were anesthetized with ketamine/xylazine [9] and blood was collected by cardiac puncture. Ear pinna were collected from just above the major ear fold. Plasma was obtained and analyzed for radioactivity using liquid scintillation techniques [9,10]. Ear tissue was digested in Solvable for 12–48 h at 60°C, as described above, and subsequently decolorized before liquid scintillation counting to determine the amount of radiolabeled lipid marker accumulation.

2.7. Corticosteroids

Two corticosteroid preparations were tested as positive controls for reducing murine ear inflammation. Mice received a 50 μg/ear dose of dexamethasone (Sigma) dissolved in acetone/olive oil (4:1, v/v). Dexamethasone was applied topically to the dorsal surface of the inflamed ear with a pipette 20 min after the ear was challenged with DNFB. Alternatively, mice were treated with Ultravate (active ingredient: halobetasol propionate, 0.05%, w/w), which was kindly donated by Dr. N. Kitson, Division of Dermatology, University of British Columbia. Ultravate, in the form of a gel, was spread evenly over the

entire dorsal surface of the target ear 20 min after DNFB challenge. To determine the effect of corticosteroids on LUV accumulation, mice received a lateral tail vein injection of 100 nm DSPC/CH (55:45) LUV, at a dose of 100 mg/kg, 15 min after corticosteroid application to the ears. At appropriate times mice were terminated and ears removed for scintillation counting as described above.

3. Results

3.1. Evaluation of ear inflammation

The most straightforward measurement used to monitor the progression of inflammation in this model is ear thickness, which reflects the presence of edema [15,17]. In ICR mice, an increase in ear thickness is measurable 6 h after DNFB challenge; it peaks at 24 h and essentially returns to normal levels after 72 h (Fig. 1, solid circles). We found this measurement to be highly reproducible as long as the protocol outlined in Section 2 is adhered to. The pinnae of untreated ears exhibited an average baseline thickness of 21 μm. At the peak of inflammation this approximately doubled to 40 μm, consistent with what has been reported previously [21]. Increases in thickness were not observed for control ears that received vehicle alone (data not shown).

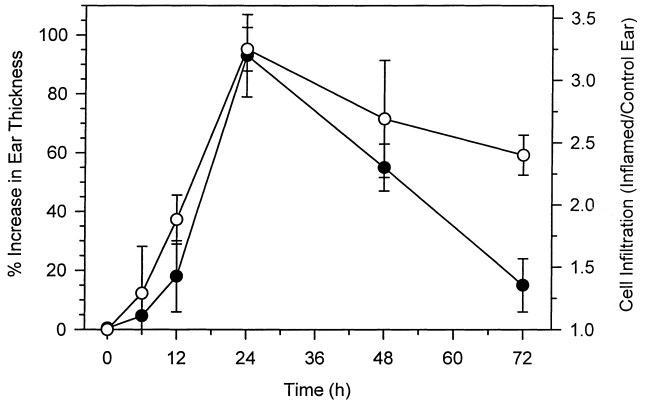

Fig. 1. Time course for ear thickness and cellular infiltration following a DNFB challenge. Mice were sensitized as described in Section 2. Three days later they were given an intraperitoneal (i.p.) injection of [^{3}H]methyl thymidine. Baseline ear measurements were made 24 h later, using an engineer's micrometer. Mice were subsequently challenged on the dorsal surface of the left ear with a 0.2% DNFB solution to initiate inflammation. At the times indicated, ear thickness (●) was measured and expressed as a percent increase over the baseline value. The mice were killed and the level of ^{3}H-labeled leukocytes measured in each ear. Cellular infiltration (○) is expressed as the ratio of radioactivity measured in the inflamed ear to the activity in the contralateral, control ear. Data are expressed as the mean ± S.D., $n=4$ animals.

The inflammatory process was also evaluated by measuring cell trafficking into the treated ear relative to the contralateral control. Bone marrow cells and circulating lymphocytes were labeled with [^{3}H]methyl thymidine as described in Section 2. Predominantly neutrophils, monocytes, and T lymphocytes begin to accumulate after a lag period of 6 h. As shown in Fig. 1 (open circles), maximum cellular influx occurs at 24 h, the same as for maximum ear thickness but infiltration levels decay more slowly than the swelling. In a similar model, Goebler et al. [22] demonstrated that the total number of infiltrating cells measured by histochemical techniques also peaked at 24 h but these cells did not completely leave the inflammation site for about 2 weeks.

3.2. Liposome accumulation at the inflammation site

Large unilamellar vesicles (LUV), composed of DSPC/CH and with a diameter of approximately 120 nm, were used to assess liposome extravasation and accumulation at the inflammation site. This type of LUV is known to be stable in blood and, at a dose of approximately 100 mg/kg, exhibits a relatively long circulation half-life in mice (Fig. 2A). However, by 24 h approximately 90% of the initial lipid dose has been cleared from the blood. A net extravasation of vesicles into treated but not untreated ears is observed during the plasma elimination phase. Vesicles administered as an i.v. bolus injection via the lateral tail vein immediately after the epicutaneous application of DNFB accumulated over the first 24 h (Fig. 2B, solid squares). The increase and subsequent decline in vesicle concentration at the inflamed site reflects the kinetics observed for changes in ear thickness and cellular infiltration (Fig. 1), peaking at 24 h but, like the thickness measurement, returning to near background levels by 72 h.

To measure the relative permeability of the vasculature to LUV during the time course of inflamma-

tion, vesicles were administered to separate groups of animals either at the time of challenge with DNFB ($t = 0$), or at 24 or 48 h post-challenge. The level of radioactivity accumulated in the ears was measured 24 h later. The data (Fig. 3) show that for this acute inflammation response, lipid accumulation in the inflamed ears occurred only during the first 24 h. The concentration of LUV in the circulation is the same for all three 24 h periods (0–24; 24–48; 48–72), but vesicles administered at 24 and 48 h post-challenge do not accumulate to any significant extent in treated ears and not at all in the control ears.

When determining liposome accumulation in an organ or at a tissue site, corrections must be made for blood volume. This is because the level of vesicles remaining in the blood pool can make a significant contribution to the total level of liposomal lipid

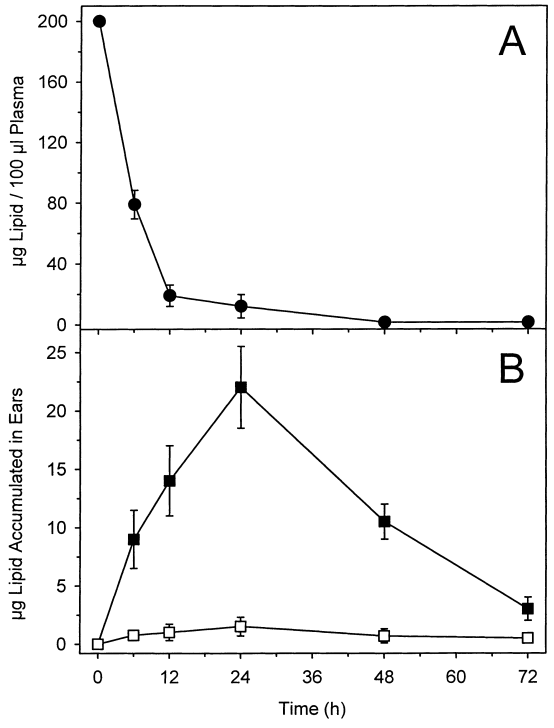

Fig. 2. The clearance of LUV from the circulation (A) and their concomitant accumulation in the inflamed ear (B). Fifteen minutes after DNFB ear challenge, mice were injected with radiolabeled vesicles, 120 nm in diameter and composed of DSPC/CH (55:45), at a dose of 100 mg/kg. At the times indicated, mice were killed and blood removed to determine the vesicle concentration remaining in plasma; data are shown in panel A (●). Inflamed (■) and noninflamed (□) ears were also removed and analyzed for lipid content (panel B). Data are expressed as the mean ± S.D., $n = 4$ animals.

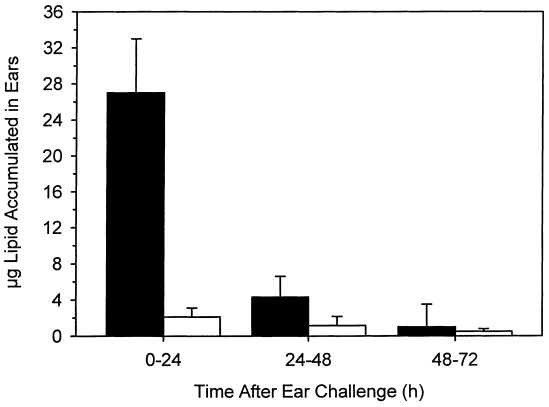

Fig. 3. Permeability of the vasculature to LUV during three 24 h intervals following DNFB ear challenge. Sensitized mice were challenged on the left ear with DNFB. Radiolabeled LUV (120 nm, 100 mg/kg) were administered by lateral tail vein injection at different stages of inflammation. One set of mice received an LUV injection immediately after ear challenge ($t = 0$ h), another set received LUV 24 h after ear challenge ($t = 24$ h), while the last group were administered LUV 48 h post-ear painting ($t = 48$ h). Liposomes were allowed to circulate for 24 h, after which time DNFB-treated ears (solid bars) and nontreated ears (open bars) were removed, digested, and analyzed for lipid accumulation (see Section 2). Data are expressed as the mean ± S.D., $n = 4$ animals.

measured in a tissue. In the experiments described here, vasodilation was present because erythema was observed almost immediately after DNFB challenge and only gradually declined in intensity over the 72 h inflammation time course. Vesicle radioactivity was hardly detectable in the plasma at 24 h (Fig. 2A), and therefore was not expected to contribute to the overall level of lipid measured in the ears at this time point. However, the following experiment was conducted to rule out this possibility. The same dose of vesicles given immediately after ear challenge ($t = 0$ h) was instead given 24 h after ear challenge ($t = 24$ h) and radioactivity in the ears was determined 2 min later. At 100 mg/kg and early time points, DSPC/CH LUV can be employed as a blood volume marker [23]. The data showed that the lipid contribution resulting from blood in the inflamed ears at 24 h was indistinguishable from that measured for the contralateral control ears (data not shown), and was approximately 20-fold less than the lipid accumulation measured in the inflamed ear during the initial 24 h interval of ear inflammation.

3.3. Effect of topical corticosteroids

Corticosteroids are known to inhibit cellular infiltration and edema in this inflammation model [15–17]. We therefore measured their effect on lipid accumulation in the target tissue. Two different corticosteroids were employed in these studies, and both exhibited the same effects. Drugs were applied 20 min after the ear was challenged with DNFB to allow the contact irritant sufficient time to diffuse into the skin. Dexamethasone was dissolved in a vehicle of acetone and olive oil (4:1, v/v) at a concentration of 5 mg/ml, and a 10 μl dose was applied to the dorsal surface of the mouse ear using a pipette. The second drug was a commercially available gel containing 0.05% (w/w) halobetasol propionate (HBP), which was spread evenly over the ear. Both drugs effectively inhibited the increase in ear thickness and significantly reduced cellular infiltration and lipid accumulation (Fig. 4).

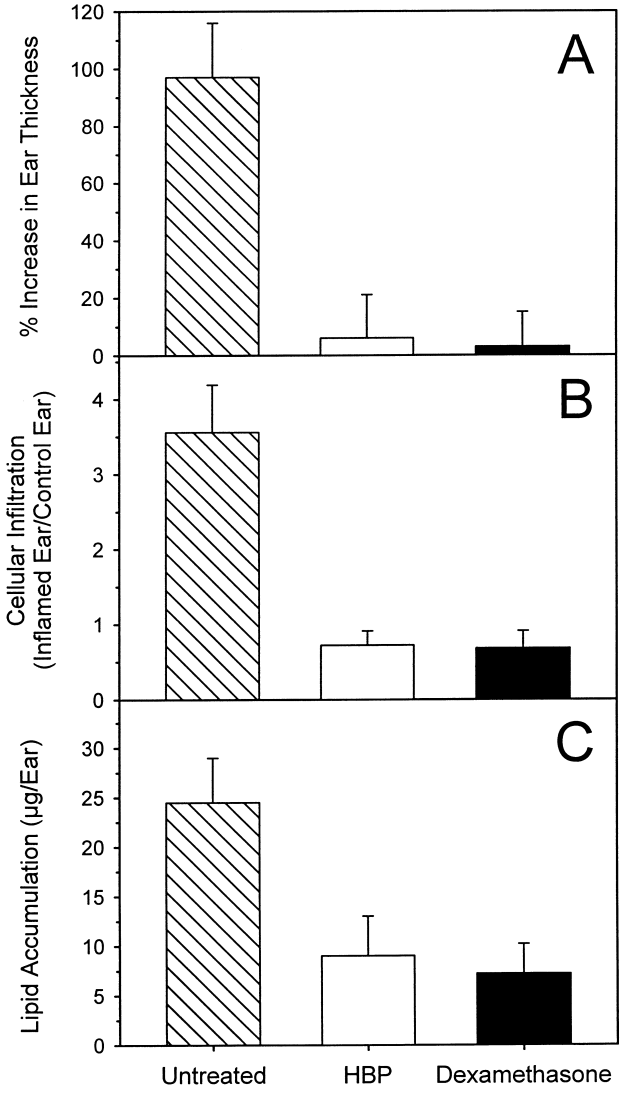

Fig. 4. Effect of topical corticosteroids on edema (A), cellular infiltration (B), and vesicle extravasation (C). Sensitized mice were challenged with DNFB; 20 min later corticosteroids were applied topically to the dorsal surface of the left ear, as described in the text. Fifteen minutes after this, mice were injected intravenously with 100 mg/kg of radiolabeled 120 nm DSPC/CH (55:45) LUV. Increase in ear thickness was determined by subtracting the baseline ear measurements from the 24 h post-ear challenge measurements. Cellular infiltration and lipid accumulation were measured as described in Section 2 and in the text. All data are expressed as the mean ± S.D., $n = 4$ animals.

3.4. Effect of vesicle size and plasma concentration on extravasation

To determine what features are important for maximizing vesicle accumulation at the inflammation site, several physical parameters were examined. Radiolabeled liposomes composed of DSPC/CH (55:45) or DSPC/CH/PEG-CerC_{20} (45:45:10) and having mean diameters of 120, 230, and 450 nm were generated using the extrusion technique [20]. Sonication of DSPC/CH LUV resulted in vesicle diameters averaging 60 nm; DSPC/CH/PEG-PegC_{20} SUV were not evaluated since, in the presence of 10 mol% PEG-lipid, it was difficult to produce vesicles with diameters less then 100 nm using the sonication procedure. These were administered immediately following DNFB ear challenge at a dose of 100 mg/kg and after 24 h the extent of lipid accumulation in the ears was measured (Fig. 5B). Additionally, the clearance kinetics of the different vesicles were examined during the 24 h period (Fig. 5A). DSPC/CH LUV with a diameter of approximately 120 nm accumulated in the inflamed ears to a level that was 2-fold greater than that observed for either the 60 or 230 nm vesicles, and at least 4-fold greater than the 450 nm vesicles (Fig. 5B, solid bars). It has been noted previously that vesicles with a mean diameter of 100 nm exhibit longer circulation times than smaller or larger vesicles with the same composition [24], and this trend was also observed here (Fig. 5A). These data suggest that there is a correlation between plasma residence time and the level of vesicle accu-

mulation in the area of inflammation. This is clearly seen from the data in Fig. 6. When DSPC/CH LUV (120 nm) are administered over a wide concentration range, to vary the circulation half-life, the area under the plasma clearance curves (plasma AUC) plotted against the area under the curve for lipid in the inflamed ear (ear AUC) shows a positive correlation. It was surprising, therefore, to observe that 120 nm

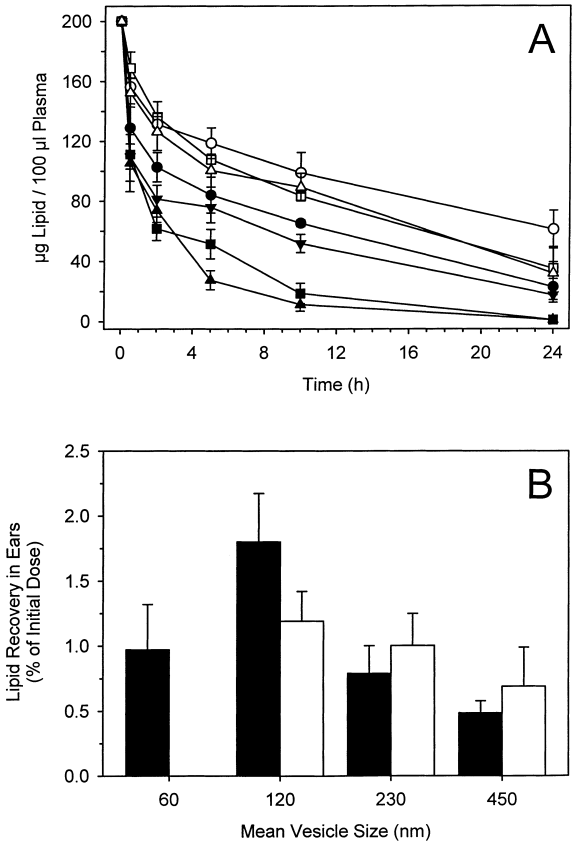

Fig. 5. The influence of vesicle size on plasma clearance kinetics (A) and extravasation at the inflammation site (B). Sensitized mice were challenged on the left ear with DNFB. Radiolabeled LUV composed of DSPC/CH (55:45 mol/mol, solid symbols and bars) or DSPC/CH/PEG-CerC_{20} (45:45:10 mol/mol, open symbols and bars) were prepared by extrusion through 100, 200, or 400 nm filters, yielding vesicles of 120 (circles), 230 (squares), and 450 (triangles) nm in diameter, respectively. Sonication was used to prepare 60 nm DSPC/CH SUV (inverted triangle), while DSPC/CH/PEG-CerC_{20} SUV were not examined. All vesicle preparations were administered via lateral tail vein injection, at a dose of 100 mg/kg. At the times indicated, plasma was removed and analyzed for radioactivity as described in the Section 2. DNFB-treated ears were removed 24 h after vesicle administration, digested, and analyzed for lipid accumulation as described previously. Data are expressed as the mean ± S.D., $n = 4$ animals.

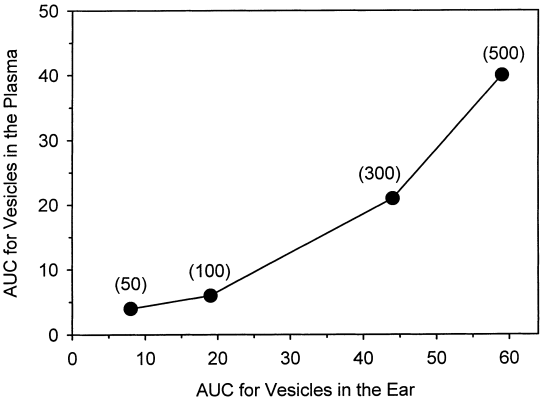

Fig. 6. Correlation between the plasma concentration of vesicles and lipid accumulation in the inflamed ear. Vesicles (DSPC/CH, 120 nm diameter) were administered at doses of 50, 100, 300, and 500 mg/kg lipid to sensitized mice 15 min after the mice were challenged with DNFB. The concentration of vesicles in both the plasma and ears was measured at 0, 6, 12, and 24 h. Profiles of the clearance and accumulation kinetics were plotted either as percent of initial dose remaining in the circulation (clearance) or µg of lipid per ear (accumulation) for the 24 h time period (each point the mean of four mice ± S.D.). The area under the curves (AUC) for each dose was measured and the data plotted.

LUV coated with polyethylene glycol (PEG) accumulated to a similar (perhaps lower) level than 120 nm uncoated vesicles (Fig. 5B, solid compared to open bars). PEG is known to inhibit the opsonization of vesicles in the circulation and increase circulation half-life [25], as is clearly shown in Fig. 5A (open symbols).

4. Discussion

The accumulation of liposomes in tumors and other disease sites, such as inflammation or infection, is an important factor in their use as clinical agents to enhance the activity of encapsulated chemotherapeutics [2,26] or to improve the diseased/normal tissue contrast ratio of imaging agents [27–30]. Thus, understanding the mechanism of vesicle extravasation and the factors that govern it will enable the design of more effective drug delivery systems. Here we have characterized the accumulation of liposomes at an inflammation site using a simple animal model of DTH. The inflammatory response was observed to be highly reproducible and inflicted a minimal level

of discomfort upon the animals. Furthermore, the development of inflammation can be monitored using several direct quantitative measurements, including ear thickness and leukocyte trafficking.

Vesicle extravasation into tumors appears to be a passive process in which circulating particles diffuse through large pores in the tumor microcirculation [31]. The hyperpermeability of the tumor vasculature is primarily dependent on the release of vascular endothelial growth factor (VEGF) by tumor cells. VEGF is responsible for promoting angiogenesis in the growing tumor. The creation of new blood vessels requires existing vessel walls to be disrupted and basement membranes to be dissolved. Endothelial cells are stimulated to proliferate and migrate, forming new capillary loops and branches [32]. However, the exact nature of the pores remains unclear and is the focus of intense research because they represent a potential route of access for drugs used in the treatment of cancer. Transport across blood vessels occurs by a variety of routes, including open gaps (interendothelial junctions and transendothelial channels), caveolae, vesicular vacuolar organelles (VVO), fenestrations, and phagocytosis. Recently, Jain and coworkers [33] showed that liposomes extravasate into subcutaneous tumors in mice via interendothelial gaps, with pore sizes ranging from 0.2 to 1.2 μm. However, the size and number of pores were observed to be dependent upon the microenvironment of the tumor, and both may be significantly reduced during tumor regression.

In the DTH model utilized for this work, recognition of the hapten DNFB by epidermal cells causes the release of proinflammatory cytokines such as interleukin-1β, interferon-γ, and tumor necrosis factor-α. These molecules induce up-regulation and increase expression of endothelial leukocyte adhesion molecule-1 (ELAM-1) and intercellular adhesion molecule-1 (ICAM-1) on the surface of endothelial cells in the local microvasculature. The adhesion molecules then bind circulating leukocytes to the endothelium. This process results in a dramatic change in blood vessel permeability [34] as the capillary vasculature undergoes structural remodeling to allow leukocyte diapedesis. Presumably, the interendothelial cell gaps that enable leukocyte extravasation also allow vesicle diffusion out of the blood compartment. This is consistent with the measured time courses for edema formation, cellular infiltration, and vascular leak as shown in Figs. 1 and 2B.

Liposomes leave the inflammation site more quickly than the cellular infiltrate. Lipid radioactivity has returned to normal levels by 72 h, but ^{3}H-labeled leukocytes remain in the skin for many days [22]. As the vascular endothelium becomes impermeable to vesicle extravasation again 24 h after DNFB contact (Fig. 3), vesicles cannot leak back into the circulation the same way they entered. However, the rate at which vesicles are cleared from the ear is similar to the rate of decrease in edema swelling measurements (Figs. 1 and 2B). Tissue clearance of the vesicles probably occurs by drainage of the vesicles into the lymphatic system along with small molecules and fluid and/or by macrophage phagocytosis, which similarly removes vesicles from tissue via the lymphatics. The cellular infiltrate leaves the inflammation site more slowly than vesicles; this may reflect the adhesive interactions that leukocytes have with dermal and epidermal cells such as keratinocytes. In this inflammation model, ICAM-1 expression on keratinocytes has been shown to peak at around 72 h and decay slowly during a 2-week period [22]. Furthermore, the increased expression of keratinocyte ICAM-1 correlates with an increased localization of T lymphocytes in the epidermis, as has been observed in chronic inflammatory skin disorders such as psoriasis [35].

If vesicle accumulation at sites of inflammation occurs by passive diffusion through interendothelial cell gaps, then the mass of lipid delivered to a particular site will be proportional to both the volume of blood passing through the tissue per unit time and the concentration of vesicles in the blood compartment (assuming that the pore size is not limiting). The vesicle concentration in plasma will be dependent upon lipid composition, dose, and vesicle diameter, as these factors influence the rate at which vesicles are cleared from the circulation. The pores are clearly large enough to allow 450 nm particles to pass through (Fig. 5), and the difference in accumulation of the different-sized vesicles most likely reflects their circulation half-lives. For example, LUV with a diameter of approximately 60 nm exhibit a larger volume of distribution in the liver than 120 nm vesicles, and as a result they tend to be cleared from the circulation more rapidly [24,36]. Small

vesicles have also been shown to diffuse from subcutaneous sites into the lymphatic system at a faster rate than large vesicles [37]. Consequently, it is possible that the 60 nm liposomes drain from the site of inflammation at a faster rate than the larger ones. The combination of these factors would be expected to result in a lower net accumulation of 60 nm vesicles at the inflammation site. On the other hand, the 230 and 450 nm systems are more readily trapped and phagocytosed by fixed macrophages of the reticuloendothelial system (RES) in the liver and spleen. The resulting shortened circulation half-lives for these large vesicles reduces their plasma concentration more quickly, which is reflected in the reduced accumulation in the inflamed ear.

It is very interesting that the PEG-coated vesicles accumulated only to the same level measured for PEG-free vesicles, and perhaps to even lower levels for the 120 nm LUV, although more studies would be necessary to ensure statistical significance. The accumulation of the different sized PEG-coated vesicles is similar, which is consistent with the plasma residence times (Fig. 5A). PEG inhibits opsonization of vesicles in plasma and slows their plasma clearance by Kupffer cells in the liver [25]. Increasing vesicle circulation lifetimes should result in an increased delivery of lipid to the inflammation site. However, despite a 1.6-fold increase in the AUC value (μg lipid in plasma over 24 h, calculated from Fig. 5A) for PEG-coated compared to naked 120 nm LUV, fewer PEG-coated vesicles accumulate. The difference is even more striking for the 450 nm liposomes; in this case PEG produces a 4.3-fold increase in plasma lipid AUC for the 24 h period, yet the accumulation of vesicles is essentially the same as for naked vesicles. Our data are similar to the observations made in a recent study which found that adding PEG to vesicles did not enhance their extravasation into the peritoneal cavity, despite increasing the plasma half-life by a factor of 2 [10]. When vesicles of the same size and composition were used in the ear inflammation model, a correlation between plasma concentration and liposome accumulation at the inflammation site was clearly seen (Fig. 6). Taken together, these data suggest that PEG may inhibit extravasation, an observation that warrants further investigation.

In conclusion, we believe that the murine model of ear inflammation is ideal for studying disease-site targeting of liposomes. The inflammation response is fast, reproducible, well defined, and easily quantified. The ear vasculature is hyperpermeable for the first 24 h following DNFB ear painting, during which time particles as large as 450 nm in diameter can extravasate into the surrounding tissue; however, maximum lipid delivery is observed for 120 nm LUV. Accumulation of lipid at the inflammation site is proportional to the plasma concentration for vesicles of the same size and composition. We are presently utilizing this model to investigate how lipid-based delivery systems can enhance the activity of systemically administered anti-inflammatory drugs.

Acknowledgements

The authors would like to thank Ms. Kym Sutton and Ms. Tina Nolan for their assistance with the animal experiments. The engineer's micrometer was kindly donated by Dr. Neil Reiner. Sandra Klimuk was supported by a grant from the Science Council of British Columbia.

References

[1] D.M. Rose, S.N. Hochwald, L.E. Harrison, M. Burt, Selective glutathione repletion with oral oxothiazolidine carboxylate (OTZ) in the radiated tumor-bearing rat, J. Surg. Res. 62 (1996) 224–228.

[2] L.D. Mayer, M.B. Bally, P.R. Cullis, S.L. Wilson, J.T. Emerman, Comparison of free and liposome encapsulated doxorubicin tumor drug uptake and antitumor efficacy in the SC115 murine mammary tumor, Cancer Lett. 53 (1990) 183–190.

[3] I.A. Bakker-Woudenberg, M.T. ten Kate, L.E. Stearne-Cullen, M.C. Woodle, Efficacy of gentamicin or ceftazidime entrapped in liposomes with prolonged blood circulation and enhanced localization in *Klebsiella pneumoniae*-infected lung tissue, J. Infect. Dis. 171 (1995) 938–947.

[4] E.A. Forssen, The design and development of Dauno-Xome(R) for solid tumor targeting in vivo, Adv. Drug Deliv. Rev. 24 (1997) 133–150.

[5] E.S. Casper, G.K. Schwartz, A. Sugarman, D. Leung, M.F. Brennan, Phase I trial of dose-intense liposome-encapsulated doxorubicin in patients with advanced sarcoma, J. Clin. Oncol. 15 (1997) 2111–2117.

[6] N.L. Boman, M.B. Bally, P.R. Cullis, L.D. Mayer, M.S. Webb, Encapsulation of vincristine in liposomes reduces its

toxicity and improves its anti-tumor efficacy, J. Liposome Res. 5 (1995) 523–541.
[7] M.S. Webb, T.O. Harasym, D. Masin, M.B. Bally, L.D. Mayer, Sphingomyelin-cholesterol liposomes significantly enhance the pharmacokinetic and therapeutic properties of vincristine in murine and human tumour models, Br. J. Cancer 72 (1995) 896–904.
[8] T.O. Harasym, P.R. Cullis, M.B. Bally, Intratumor distribution of doxorubicin following i.v. administration of drug encapsulated in egg phosphatidylcholine/cholesterol liposomes, Cancer Chemother. Pharmacol. 40 (1997) 309–317.
[9] M.J. Parr, D. Masin, P.R. Cullis, M.B. Bally, Accumulation of liposomal lipid and encapsulated doxorubicin in murine Lewis lung carcinoma: The lack of beneficial effects by coating liposomes with poly(ethylene glycol), J. Pharmacol. Exp. Ther. 280 (1997) 1319–1327.
[10] S.A. Longman, P.G. Tardi, M.J. Parr, L. Choi, P.R. Cullis, M.B. Bally, Accumulation of protein-coated liposomes in an extravascular site: Influence of increasing carrier circulation lifetimes, J. Pharmacol. Exp. Ther. 275 (1995) 1177–1184.
[11] M.B. Bally, D. Masin, R. Nayar, P.R. Cullis, L.D. Mayer, Transfer of liposomal drug carriers from the blood to the peritoneal cavity of normal and ascitic tumor-bearing mice, Cancer Chemother. Pharmacol. 34 (1994) 137–146.
[12] N.Z. Wu, D. Da, T.L. Rudoll, D. Needham, A.R. Whorton, M.W. Dewhirst, Increased microvascular permeability contributes to preferential accumulation of Stealth liposomes in tumor tissue, Cancer Res. 53 (1993) 3765–3770.
[13] F. Yuan, M. Leunig, S.K. Huang, D.A. Berk, D. Papahadjopoulos, R.K. Jain, Microvascular permeability and interstitial penetration of sterically stabilized (stealth) liposomes in a human tumor xenograft, Cancer Res. 54 (1994) 3352–3356.
[14] E.A. Forssen, R. Male-Brune, J.P. Adler-Moore, M.J.A. Lee, P.G. Schmidt, T.B. Krasieva, S. Shimizu, B.J. Tromberg, Fluorescence imaging studies for the disposition of daunorubicin liposomes (DaunoXome) within tumor tissue, Cancer Res. 56 (1996) 2066–2075.
[15] J.M. Young, L.M. De Young, Cutaneous models of inflammation for the evaluation of topical and systemic pharmacological agents, in: J.Y. Chang, J.A. Lewis (Eds.), Pharmacological Methods in the Control of Inflammation, Alan R. Liss, New York, 1989, pp. 215–231.
[16] R. Niedner, Animal models, in: H.I. Maibach, C. Surber (Eds.), Topical Corticosteroids, Karger, Basel, 1992, pp. 7–16.
[17] J.R. Chapman, Z. Ruben, G.M. Butchko, Histology of and quantitative assays for oxazolone-induced allergic contact dermatitis in mice, Am. J. Dermatopathol. 8 (1986) 130–138.
[18] A. van de Stolpe, P.T. van der Saag, Intercellular adhesion molecule-1, J. Mol. Med. 74 (1996) 13–33. (Review)
[19] J.M. Young, D.A. Spires, C.J. Bedord, B. Wagner, S.J. Ballaron, L.M. De Young, The mouse ear inflammatory response to topical arachidonic acid, J. Invest. Dermatol. 82 (1984) 367–371.
[20] M.J. Hope, M.B. Bally, G. Webb, P.R. Cullis, Production of large unilamellar vesicles by a rapid extrusion procedure. Characterization of size distribution, trapped volume and ability to maintain a membrane potential, Biochim. Biophys. Acta 812 (1985) 55–65.
[21] P.L. Chisholm, C.A. Williams, R.R. Lobb, Monoclonal antibodies to the integrin alpha-4 subunit inhibit the murine contact hypersensitivity response, Eur. J. Immunol. 23 (1993) 682–688.
[22] M. Goebeler, J. Gutwald, J. Roth, G. Meinardus-Hager, C. Sorg, Expression of intercellular adhesion molecule-1 in murine allergic contact dermatitis, Int. Arch. Allergy Appl. Immunol. 93 (1990) 294–299.
[23] M.B. Bally, L.D. Mayer, M.J. Hope, R. Nayar, Pharmacodynamics of liposomal drug carriers: methodological considerations, in: G. Gregoriadis, (Ed.), Liposome Technology, CRC Press, Boca Raton, 1993, pp. 27–41.
[24] W.V. Rodrigueza, P.H. Pritchard, M.J. Hope, The influence of size and composition on the cholesterol mobilizing properties of liposomes in vivo, Biochim. Biophys. Acta 1153 (1993) 9–19.
[25] D. Papahadjopoulos, T.M. Allen, A. Gabizon, E. Mayhew, K. Matthay, S.K. Huang, K.D. Lee, M.C. Woodle, D.D. Lasic, C. Redemann, Sterically stabilized liposomes: improvements in pharmacokinetics and antitumor therapeutic efficacy, Proc. Natl. Acad. Sci. U.S.A. 88 (1991) 11460–11464.
[26] E.A. Forssen, D.M. Coulter, R.T. Proffitt, Selective in vivo localization of daunorubicin small unilamellar vesicles in solid tumors, Cancer Res. 52 (1992) 3255–3261.
[27] O.C. Boerman, W.J.G. Oyen, G. Storm, M.L. Corvo, L. van Bloois, J.W.M. Van der Meer, F.H.M. Corstens, Technetium-99m labelled liposomes to image experimental arthritis, Ann. Rheum. Dis. 56 (1997) 369–373.
[28] I. Ogihara, S. Kojima, M. Jay, Differential uptake of gallium-67-labeled liposomes between tumors and inflammatory lesions in rats, J. Nucl. Med. 27 (1986) 1300–1307.
[29] C.A. Presant, A.F. Turner, R.T. Proffitt, Potential for improvement in clinic decision-making: tumor imaging with in-111 labeled liposomes results of a phase II–III study, J. Liposome Res. 4 (1994) 985–1008.
[30] C. Tilcock, Liposomal blood pool agents for nuclear medicine and magnetic resonance imaging, J. Liposome Res. 4 (1994) 909–936.
[31] F. Yuan, M. Dellian, D. Fukumura, M. Leunig, D.A. Berk, V.P. Torchilin, R.K. Jain, Vascular permeability in a human tumor xenograft: molecular size dependence and cutoff size, Cancer Res. 55 (1995) 3752–3756.
[32] R.K. Jain, K. Schlenger, M. Hockel, F. Yuan, Quantitative angiogenesis assays: progress and problems, Nature Med. 3 (1997) 1203–1208. (Review)
[33] S.K. Hobbs, W.L. Mosky, F. Yuan, W.G. Roberts, L. Griffith, V.P. Torchilin, R.K. Jain, Regulation of transport pathways in tumor vessels: Role of tumor type and microenvironment, Proc. Natl. Acad. Sci. U.S.A. 95 (1998) 4607–4612.

[34] B.C. Marcus, K.L. Hynes, B.L. Gewertz, Loss of endothelial barrier function requires neutrophil adhesion, Surgery 122 (1997) 420–426.
[35] J.N. Barker, Adhesion molecules in cutaneous inflammation, Ciba Found. Symp. 189 (1995) 91–101. (Review)
[36] W.V. Rodrigueza, S.K. Klimuk, P.H. Pritchard, M.J. Hope, Cholesterol mobilization and regression of atheroma in cholesterol-fed rabbits induced by large unilamellar vesicles, Biochim. Biophys. Acta 1368 (1998) 306–320.
[37] C. Oussoren, J. Zuidema, D.J.A. Crommelin, G. Storm, Lymphatic uptake and biodistribution of liposomes after subcutaneous injection.2. Influence of liposomal size, lipid composition and lipid dose, Biochim. Biophys. Acta 1328 (1997) 261–272.